

Cite this: *Chem. Sci.*, 2023, **14**, 5188

All publication charges for this article have been paid for by the Royal Society of Chemistry

Molybdenum carbonyl assisted reductive tetramerization of CO by activated magnesium(I) compounds: squareate dianion vs. metallo-ketene formation†

K. Yuvaraj, ‡^a Jeremy C. Mullins, ^a Thayalan Rajeshkumar, ^b Iskander Douair, Laurent Maron *^b and Cameron Jones *^a

Reactions of a dimagnesium(I) compound, $\{(\text{Dip}^{\text{Dip}}\text{Nacnac})\text{Mg}\}_2$ ($\text{Dip}^{\text{Dip}}\text{Nacnac} = [\text{HC}(\text{MeCNDip})_2]^-$, Dip = 2,6-diisopropylphenyl), pre-activated by coordination with simple Lewis bases (4-dimethylaminopyridine, DMAP; or TMC, :C(MeNCMe)₂), with 1 atmosphere of CO in the presence of one equivalent of $\text{Mo}(\text{CO})_6$ at room temperature, led to the reductive tetramerisation of the diatomic molecule. When the reactions were carried out at room temperature, there is an apparent competition between the formation of magnesium squareate, $\{(\text{Dip}^{\text{Dip}}\text{Nacnac})\text{Mg}\}\{\text{cyclo-}(\kappa^4\text{-C}_4\text{O}_4)\}\{\mu\text{-Mg}(\text{Dip}^{\text{Dip}}\text{Nacnac})\}_2$, and magnesium metallo-ketene products, $\{(\text{Dip}^{\text{Dip}}\text{Nacnac})\text{Mg}\}\{\mu\text{-O=CC}(\text{Mo}(\text{CO})_5)\text{C}(\text{O})\text{CO}_2\}\{\text{Mg}(\text{D})\}(\text{Dip}^{\text{Dip}}\text{Nacnac})\}$, which are not interconvertible. Repeating the reactions at 80 °C led to the selective formation of the magnesium squareate, implying that this is the thermodynamic product. In an analogous reaction, in which THF is the Lewis base, only the metallo-ketene complex, $\{(\text{Dip}^{\text{Dip}}\text{Nacnac})\text{Mg}\}\{\mu\text{-O=CC}(\text{Mo}(\text{CO})_5)\text{C}(\text{O})\text{CO}_2\}\{\text{Mg}(\text{THF})\}(\text{Dip}^{\text{Dip}}\text{Nacnac})\}$ is formed at room temperature, while a complex product mixture is obtained at elevated temperature. In contrast, treatment of a 1:1 mixture of the guanidinato magnesium(I) complex, $\{(\text{Priso})\text{Mg}-\text{Mg}(\text{Priso})\}$ (Priso = $[\text{Pr}'_2\text{NC}(\text{NDip})_2]^-$), and $\text{Mo}(\text{CO})_6$, with CO gas in a benzene/THF solution, gave a low yield of the squareate complex, $\{(\text{Priso})(\text{THF})\text{Mg}\}\{\text{cyclo-}(\kappa^4\text{-C}_4\text{O}_4)\}\{\mu\text{-Mg}(\text{THF})(\text{Priso})\}_2$, at 80 °C. Computational analyses of the electronic structure of squareate and metallo-ketene product types corroborate the bonding proposed from experimental data, for the C_4O_4 fragments of these systems.

Received 22nd March 2023
Accepted 24th April 2023

DOI: 10.1039/d3sc01487h
rsc.li/chemical-science

Introduction

Carbon monoxide is produced on an industrial scale by processes including the partial oxidation of methane, and the gasification of coal or biomass.¹ The gas is used as a C₁ feedstock in a variety of processes, which produce value-added commodity chemicals on mega-tonne scales per annum. Of most relevance to this study is the Fischer-Tropsch process (FT), which transforms mixtures of CO and H₂ (syngas) into liquid hydrocarbons and oxygenates, typically in the presence of heterogeneous transition metal catalysts, and under elevated temperatures and pressures.² While little success has been had

catalysing FT under homogeneous conditions, a great deal of work has centred on the use of organometallic compounds to study the fundamental steps of this process in solution.³ Such studies have led to a growing understanding of how the very strong bond in CO (BDE = 257 kcal mol⁻¹)⁴ can be activated and functionalized by reactive metal centres.

With respect to the study of C–C bond forming processes, the reductive homologation of CO into a good number of cyclic and acyclic C–C coupled oxo-carbon anions, $[\text{C}_m\text{O}_m]^{n-}$ ($m, n > 1$), has been achieved by reaction of the gas with low-valent complexes involving electropositive elements from the p, d- and f-blocks of the periodic table.⁵ In 2019 we extended this work to the s-block for the first time, with the reductive trimerization of CO to the deltate complex **1** (Fig. 1), by dimagnesium(I) complexes $\{(\text{Dip}^{\text{Dip}}\text{Nacnac})\text{Mg}-\text{Mg}(\text{D})\}(\text{Dip}^{\text{Dip}}\text{Nacnac})$ ($\text{Dip}^{\text{Dip}}\text{Nacnac} = [\text{HC}(\text{MeCNDip})_2]^-$, Dip = 2,6-diisopropylphenyl; D = Lewis base), which were activated by coordination of one Mg center with a simple Lewis base.^{6,7} It is of note that in the absence of Lewis bases (D), three-coordinate dimagnesium(I) compounds, $[\text{LMg}-\text{MgL}]$ (L = β-diketiminate or guanidinate), are unreactive towards CO under ambient conditions.⁶ The only other report of deltate formation from

^aSchool of Chemistry, Monash University, PO Box 23, VIC, 3800, Australia; Web: <http://www.monash.edu/science/research-groups/chemistry/jonesgroup>. E-mail: cameron.jones@monash.edu; https://twitter.com/Jones_Research

^bUniversité de Toulouse et CNRS, INSA, UPS, LPCNO, UMR 5215, 135 Avenue de Rangueil, F-31077 Toulouse, France. E-mail: laurent.maron@irsamc.ups-tlse.fr

† Electronic supplementary information (ESI) available. CCDC 2250277–2250283.

For ESI and crystallographic data in CIF or other electronic format see DOI: <https://doi.org/10.1039/d3sc01487h>

‡ Current address: Department of Chemistry, Indian Institute of Technology Palakkad, Palakkad-678557, Kerala, India.



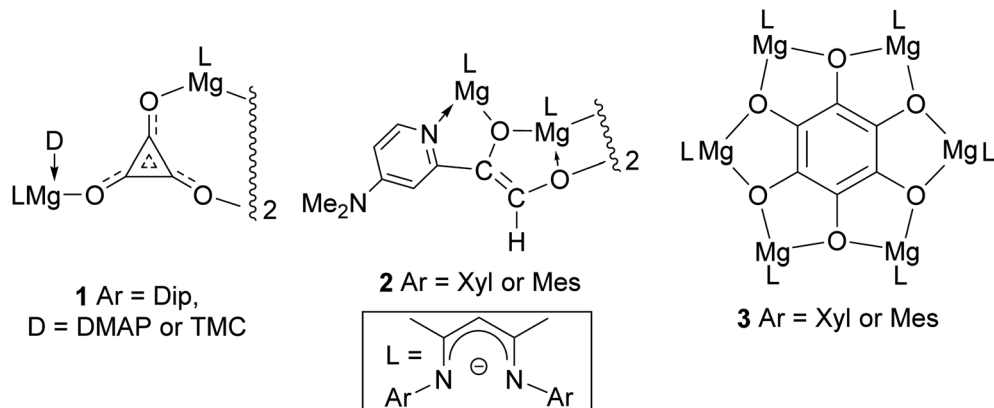


Fig. 1 Previously described products derived from the reductive homologation of CO by neutral dimagnesium(i) compounds.

CO reduction came from Cloke and co-workers, who used a uranium(III) complex as the reductant.⁸ They, and others, later showed that ethynediolate and squareate ($[C_mO_m]^{2-}$, $m = 2$ and 4 respectively) complexes can also be selectively accessed by altering the steric profile of the f-block organometallic reductant.⁹ In a similar vein, when we reacted the less bulky dimagnesium(i) compounds $[(^{Ar}Nacnac)Mg-Mg(DMAP)(^{Ar}Nacnac)]$ ($Ar = \text{mesityl (Mes)} \text{ or } 2,6\text{-xylyl (Xyl)}$; DMAP = 4-dimethylaminopyridine) with CO, reductive dimerization of the gas to $[C_2O_2]^{2-}$, followed by C–H activation of DMAP, yielded the ethenediolates, 2.^{10,11}

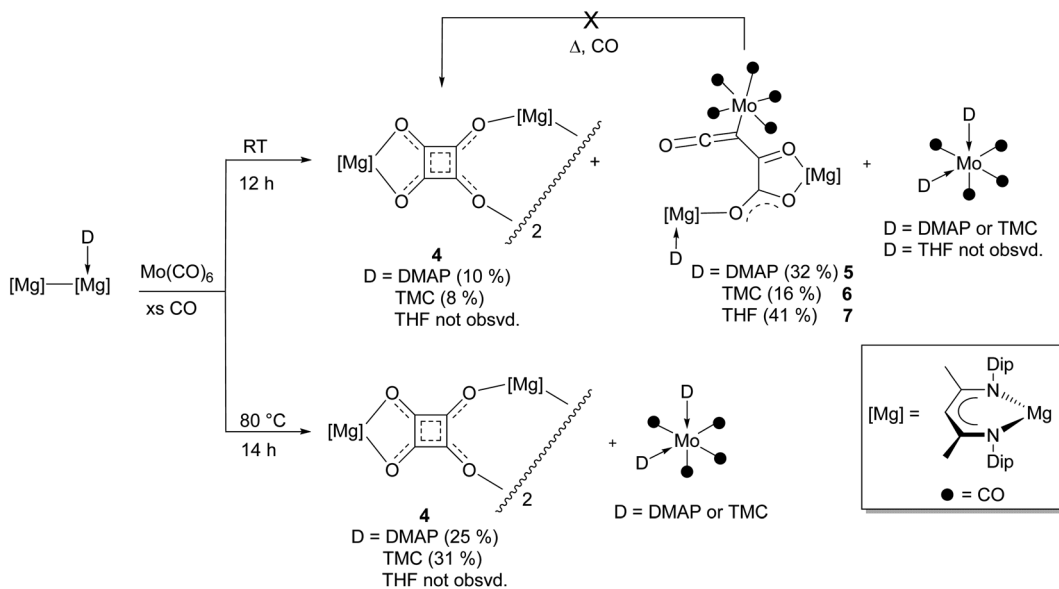
As an alternative to Lewis base activation of dimagnesium(i) compounds, we have shown that cooperative heterobimetallic strategies for CO homologation are effective. For example, treating $[(^{Ar}Nacnac)Mg-Mg(^{Ar}Nacnac)]$ ($Ar = \text{Xyl or Mes}$) with CO in the presence of catalytic $Mo(CO)_6$ led to reductive hexamerization of the gas, and formation of the benzenehexolate complexes, 3.¹² These represented the first well-defined benzenehexolate complexes derived from CO, though it is noteworthy that $K_6C_6O_6$ was proposed by Liebig to have been formed in the reaction between molten potassium and CO, as long ago as 1834.¹³ Given our success using dimagnesium(i) compounds for the selective reductive dimerization, trimerization and hexamerization of CO, we were keen to explore routes to other C–C coupled oligomers of the diatomic molecule. We were especially interested in squareate formation, $[C_4O_4]^{2-}$, given the results of a recent study that showed $MgCl^-$ to reduce CO to squareate in the gas phase.¹⁴ Here, we reveal that by combining dimagnesium(i) activation by simple Lewis base coordination, and a cooperative heterobimetallic strategy, selective reductive tetramerizations of CO can, indeed, be achieved. The two CO derived product types obtained using this approach, magnesium squareates and magnesium metallo-glyoxylato ketenes (hereafter, on occasion, abbreviated as metallo-ketenes), are unprecedented as isolated species. Moreover, the distribution of the two products can be readily altered by manipulating the reaction conditions. The electronic structure of the products of these reactions has been explored using DFT calculations.

Results and discussion

At the outset of this study the reaction between $[(^{Dip}Nacnac)Mg-Mg(DMAP)(^{Dip}Nacnac)]$ and CO, in the presence of 25 mol% $Mo(CO)_6$, was carried out at room temperature. This led to isolation of low yields of the colourless squareate and orange metallo-ketene complexes, 4 and 5 respectively, in addition to a trace of magnesium deltate 1 ($D = \text{DMAP}$) (Scheme 1). This result shows that, unlike for the synthesis of benzenehexolate 3, $Mo(CO)_6$ is largely consumed in the reaction and does not act as a catalyst, at least in the formation of 5. As a result, the reaction was repeated, but using one equivalent of $Mo(CO)_6$. This led to increased isolated yields of 4 and 5 (and no 1), with 5 being the predominant product. Similar reactions were subsequently carried out with TMC ($:C(MeNCMe)_2$) and THF adducts of the dimagnesium(i) compound.¹⁵ The former gave a mixture of squareate 4 and metallo-ketene 6, whereas only the metallo-ketene 7 was isolated from the latter reaction, and no squareate 4 was observed in the reaction mixture (as determined by an ^1H NMR spectroscopic analysis). In order to determine if the metallo-ketene products, 5–7, are intermediates in the formation of squareate, 4, benzene solutions of the compounds were heated to 80 °C under atmospheres of CO. In no case was squareate 4 formed, suggesting a competition exists between distinct reaction pathways to the squareate and metallo-ketene products. That the metallo-ketenes do not convert to squareate 4 is perhaps not surprising, considering that the formation of the former must involve at least one $C\equiv O$ bond cleavage. Transformation to 4 would require O-migration through formal C–O bond cleavage and formation steps, ring closure through formation of a C–C bond, and loss of the $Mo(CO)_5$ Lewis base fragment.

So as to determine if the product distributions obtained from the reactions involving DMAP and TMC activated systems are affected by reaction temperature, they were repeated, but with heating at 80 °C overnight. In both cases squareate 4 was isolated in higher yields than obtained for the corresponding room temperature reactions, and no metallo-ketene products were recovered. This may indicate that squareate 4 is the



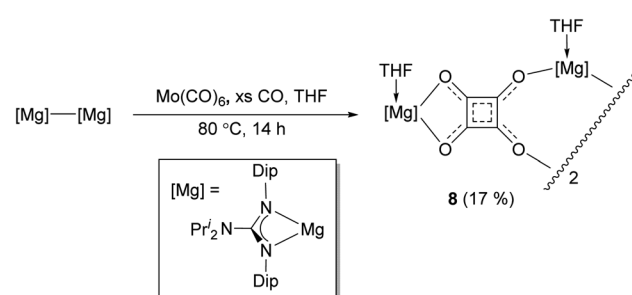


Scheme 1 Synthesis of compounds 4–7 at either room temperature or 80 °C (isolated yields given in parentheses).

thermodynamic product, whereas metallo-ketenes 5 and 6 are kinetic products. In addition, the fate of the molybdenum carbonyl, and DMAP and TMC Lewis bases, in the formation of 4 appears to be generation of the *cis*-adducts $[\text{Mo}(\text{CO})_4(\text{D})_2]$ (D = DMAP or TMC), which were isolated from the respective reactions, and crystallographically characterised. These compounds were subsequently rationally synthesized and spectroscopically characterised, which allowed confirmation that they are also low yield products in the associated reactions carried out at room temperature. Moreover, the formation of stable *cis*- $[\text{Mo}(\text{CO})_4(\text{D})_2]$ seemingly shuts down any catalytic activity of $\text{Mo}(\text{CO})_6$, as was important in the formation of magnesium benzenehexolate 3.¹²

It is interesting that no squarate complex was formed in the reaction that gave 7. Indeed, when that reaction was repeated at elevated temperature, squarate 4 was again not isolated from the reaction mixture, which an ¹H NMR spectroscopic analysis showed to contain a complex mixture of products. The differences with the reactions involving DMAP or TMC activated dimagnesium(i) compounds might stem from the fact that *cis*- $[\text{Mo}(\text{CO})_4(\text{THF})_2]$ is not a stable compound (see below), whereas the stability of *cis*- $[\text{Mo}(\text{CO})_4(\text{D})_2]$ (D = DMAP or TMC) might help drive formation of squarate 4. To explore this further, $[(\text{DipNa}^+ \text{acnac})\text{Mg—Mg}(\text{DipNa}^+ \text{acnac})]$ was substituted with the related guanidinate coordinated system $[(\text{Priso})\text{Mg—Mg}(\text{Priso})]$ ($\text{Priso} = [\text{Pr}_2\text{N}(\text{NDip})_2]^-$)¹⁶ in a potentially THF activated reaction.¹⁷ Although a reaction did occur at room temperature, it was very slow, with only a fraction of the dimagnesium(i) compound being consumed overnight. However, repeating the reaction at 80 °C overnight, afforded a low yield (17%) of the colourless THF coordinated squarate compound 8, upon work-up (Scheme 2). It is not known why squarate formation occurs, whereas it does not in the reaction involving $[(\text{DipNa}^+ \text{acnac})\text{Mg—Mg}(\text{DipNa}^+ \text{acnac})]$ in the presence of THF. The fact that the Mg centres in 8 are THF coordinated is likely a result of them being more sterically accessible than those in squarate complex 4.

Once crystallised, squarate 4 is poorly soluble in non-coordinating deuterated solvents, and decomposes upon attempts to dissolve it in neat d_8 -THF. As a result, meaningful solution state ¹³C{¹H} NMR spectroscopic data could not be obtained. Despite the ¹H NMR spectrum of the compound in d_6 -benzene displaying very broad signals, the spectral pattern is consistent with its solid-state structure. Similarly, the guanidinato-magnesium squarate complex 8 is poorly soluble in d_6 -benzene and d_8 -toluene, though ¹H and ¹³C{¹H} NMR spectra of the compound, contaminated with significant amounts of the soluble guanidine decomposition product, PrisoH,¹⁶ were obtained and tentatively assigned. No signals for the squarate carbon centres were observed in the ¹³C{¹H} NMR spectrum, so the compound was prepared under an atmosphere of ¹³CO, and the spectrum acquired before work-up. This showed two signals at δ 231.4 and 237.7 ppm, which were assigned to two inequivalent sets of $[\text{C}_4\text{O}_4]^{2-}$ carbon centres, as would be expected if the compound retained its solid-state structure in solution. It is noteworthy that the only molybdenum carbonyl signal observed in this spectrum was for $\text{Mo}(\text{CO})_6$ ($\delta = 201.3$ ppm), though the presence of other



Scheme 2 Synthesis of compound 8 (isolated yield given in parentheses).

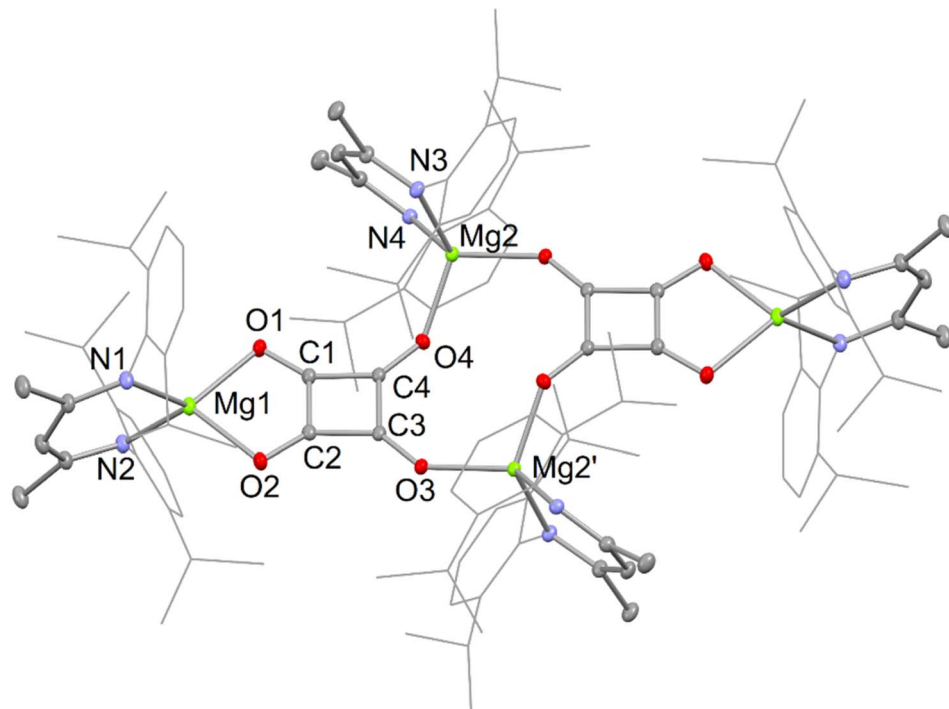


Fig. 2 Molecular structure of **4** (25% thermal ellipsoids; hydrogen atoms omitted; Dip substituents shown as wire-frame for sake of clarity). Selected bond lengths (Å) and angles (°): Mg(1)–O(2) 2.056(3), Mg(1)–O(1) 2.079(2), O(1)–C(1) 1.259(4), C(1)–C(2) 1.430(5), C(1)–C(4) 1.464(4), Mg(2)–O(4) 1.935(2), Mg(2)'–O(3) 1.953(2), O(2)–C(2) 1.259(4), C(2)–C(3) 1.463(4), O(3)–C(3) 1.244(4), C(3)–C(4) 1.473(4), O(4)–C(4) 1.244(4), O(2)–Mg(1)–O(1) 88.16(9), C(3)–O(3)–Mg(2)' 138.5(2), C(4)–O(4)–Mg(2) 143.2(2).

insoluble molybdenum carbonyl products in the reaction suspension cannot be ruled out (*e.g.* as resulting from the decomposition of the transiently generated, and unstable by-product $\text{Mo}(\text{CO})_4(\text{THF})_2$, *cf.* stable $[\text{Mo}(\text{CO})_4(\text{D})_2]$; D = DMAP or TMC; isolated when **4** was prepared in the presence of DMAP or TMC).

As was the case for **4**, the ^1H NMR spectra of the metallocetene complexes **5–7**, each exhibit sets of signals for two chemically inequivalent $^{\text{Dip}}\text{NaCNac}$ ligands, as would be expected for the solid-state structures of the compounds being preserved in solution. The poor solubility of the compounds hampered the acquisition of $^{13}\text{C}\{^1\text{H}\}$ NMR spectra of sufficient quality to enable the assignment of signals for the carbon centres of the central C_4O_4 fragment. Accordingly, compound **7** was prepared under an atmosphere of ^{13}CO , and its $^{13}\text{C}\{^1\text{H}\}$ NMR spectrum recorded as a d_6 -benzene solution. That enabled doublet signals at δ 167.6 and 190.4 ppm ($^1J_{\text{CC}} = 61$ Hz) to be assigned to the backbone carbons of the C_2O_3 glyoxylato fragment (C(1) and C(2) in the solid-state structure, see ESI \dagger), while the ketene carbon, $\text{C}=\text{C}=\text{O}$, was tentatively assigned as a singlet δ 170.3 ppm. No resonance was observed for the Mo coordinated ketenyl carbon ($\text{MoC}=\text{C}=\text{O}$), perhaps due to signal broadening. It is noteworthy that the doublet signals were superimposed on singlet resonances, of similar intensity, at their centre point. This confirms that the two carbons giving rise to those signals can originate from either ^{13}CO or $\text{Mo}^{(12)}\text{CO}_6$. This is likely also the case for the other carbons of the C_4O_4 unit. Further to this, the intensity of the ^{13}C NMR signals for the coordinated $\text{Mo}(\text{CO})_5$ unit reveal that appreciable

^{13}CO for ^{12}CO substitution within that unit has occurred during the reaction.

The X-ray crystal structures of squareate complexes **4** and **8** were determined, and their molecular structures are depicted in Fig. 2 and 3, respectively. They are both dimers in which dianionic squareate units are bridged by four-coordinate ($^{\text{Dip}}\text{NaCNac}$)Mg or five-coordinate (Priso)(THF)Mg cations, giving rise to non-planar $\text{C}_4\text{O}_4\text{Mg}_2$ ten-membered rings. In addition, each squareate fragment chelates another magnesium centre. The C–C and C–O bond lengths within each of the planar squareate moieties are similar, and lie between those normally seen for single and double bonds. This strongly suggests significant delocalisation over the $[\text{C}_4\text{O}_4]^{2-}$ units, as has been proposed by Cloke and co-workers for related uranium(IV) squareates, *e.g.* $[[\text{U}(\eta\text{-C}_5\text{H}_6\text{SiPr}_3^i)_2\text{-}1,4)(\eta\text{-C}_5\text{Me}_4\text{H})_2](\mu\text{-}\kappa^2\text{-C}_4\text{O}_4)]^{9a}$.

In the solid state, compounds **5–7** are essentially isostructural. Accordingly, only the molecular structure of one of these, **6**, is depicted in Fig. 4, while those of the other two can be found in the ESI \dagger . The compounds include a central C_4O_4 fragment which is κ^1 -coordinated to $\text{Mo}(\text{CO})_5$ and ($^{\text{Dip}}\text{NaCNac}$)(D)Mg (D = DMAP, TMC or THF) units, while also chelating a ($^{\text{Dip}}\text{NaCNac}$)Mg cation. We are unaware of any structurally characterised C_4O_4 units, similar to those in **5–7**, which can be considered as glyoxylato-ketenes. While unique, they are closely related to several f-block carboxylato-ketene complexes formed by reductive trimerisation of CO, *e.g.* $[(\text{Cp}^{\text{ttt}}\text{Tm})_2(\mu\text{-O}_2\text{C}-\text{C}=\text{O})]$ ($\text{Cp}^{\text{ttt}} = [\text{C}_5\text{H}_2\text{Bu}_3^t\text{-}1,2,4]^-$) 18 . Indeed, the glyoxylato-ketene unit in **5–7** can be viewed as the product of a formal insertion of CO into the C–C single bond of the carboxylato-ketene

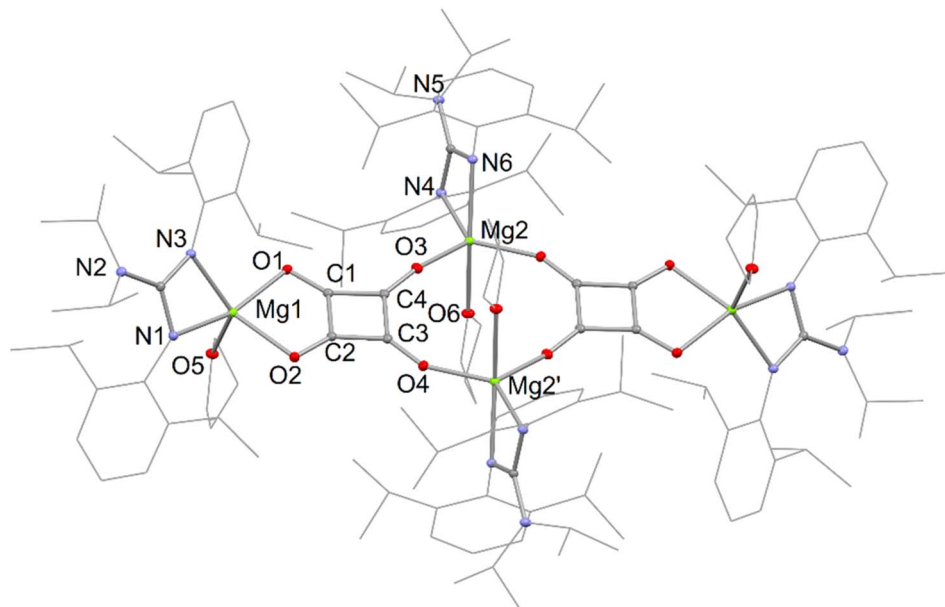


Fig. 3 Molecular structure of **8** (25% thermal ellipsoids; hydrogen atoms omitted; Dip, THF, and isopropyl substituents shown as wire-frame for sake of clarity). Selected bond lengths (Å) and angles (°): Mg(1)–O(5) 2.0285(12), Mg(1)–O(2) 2.0853(12), Mg(1)–O(1) 2.1468(12), O(1)–C(1) 1.2606(17), C(1)–C(2) 1.4384(19), C(1)–C(4) 1.465(2), Mg(2)–O(3) 1.9378(12), Mg(2)’–O(4) 1.9535(12), O(2)–C(2) 1.2616(17), C(2)–C(3) 1.461(2), O(3)–C(4) 1.2484(17), C(3)–O(4) 1.2445(18), C(3)–C(4) 1.475(2), O(2)–Mg(1)–O(1) 86.92(5), C(4)–O(3)–Mg(2) 168.16(10), C(3)–O(4)–Mg(2)’ 155.73(10).

fragment, as found in $[(Cp^{t\bar{t}t}Tm)_2(\mu-O_2C-C\equiv C=O)]$. An examination of the bond lengths within the C_4O_4 fragment is instructive. There appears to be significant electronic delocalisation over the $C(1)O_2$ unit, while the $C(1)$ – $C(2)$ bond is clearly single, signifying carboxylate-character within that C_2O_2 moiety. Interestingly, the bond lengths within the C_3O_2 fragment containing $C(3)$ are indicative of some charge delocalisation over that fragment, which could be viewed as a metallo-ketene (as depicted in Scheme 1), or as having partial carbenic character at $C(3)$, with a build up of negative charge at $O(3)$ [cf. Crimmin’s $\{(^{Dip}Nacnac)Al\}_2\{(\mu-C_4O_4)M(CO)_5\}$, $M = Mo$ or W ,¹⁹ complexes derived from Al^1 induced CO tetramerisation]. In this respect, the C – Mo distance in **6** is at the upper end of the range for reported $(CO)_5Mo$ – $C_{(3-coord)}$ bond lengths.²⁰

Despite significant efforts, the complexity of the four-component reactions that gave **4**–**7** thwarted our attempts to compute cogent reaction pathways to these compounds. However, the nature of the bonding in complexes **4** and **6** was investigated at the DFT level (B3PW91), as this methodology has already been successfully applied to describe CO homologation in other metal systems.^{6,7,9,12} The optimized geometry of compound **4** compares well with that displayed in the solid state. For example, the C–C and C–O bonds within the squarate moiety are perfectly reproduced (1.46 and 1.24 Å). These distances are in line with a significant degree of electronic delocalisation over the C_4O_4 units. The latter was corroborated by a Natural Bonding Orbital (NBO) analysis. The associated Wiberg Bond Indexes (WBI) for the C–O units are 1.40, indicating a strong covalent character to those bonds. The somewhat reduced C–O WBI, relative to what would be expected for localised $C\equiv O$ double bonds, is partially explained by some

delocalization of the CO electron density onto an empty orbital on Mg, as highlighted in the second order donor-acceptor NBO level. The CO π bond is also found to be delocalized onto the C_4

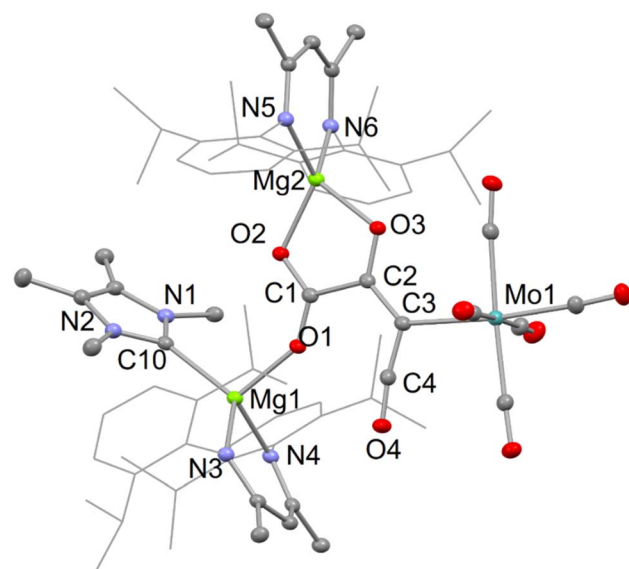


Fig. 4 Molecular structure of **6** (25% thermal ellipsoids are shown; hydrogen atoms omitted; Dip substituents shown as wireframe for sake of clarity). Selected bond lengths (Å) and angles (°): Mo(1)–C(3) 2.331(3), Mg(1)–C(10) 2.226(3), O(1)–C(1) 1.248(3), C(1)–O(2) 1.258(3), C(1)–C(2) 1.546(3), C(2)–O(3) 1.273(3), C(2)–C(3) 1.384(3), C(3)–C(4) 1.325(4), O(4)–C(4) 1.157(3), O(1)–C(1)–O(2) 126.2(2), O(1)–C(1)–C(2) 117.9(2), O(2)–C(1)–C(2) 115.8(2), O(3)–C(2)–C(3) 125.2(2), O(3)–C(2)–C(1) 113.9(2), C(3)–C(2)–C(1) 120.9(2), C(4)–C(3)–C(2) 121.5(2), C(4)–C(3)–Mo(1) 108.32(18), C(2)–C(3)–Mo(1) 129.80(18), O(4)–C(4)–C(3) 170.8(3).

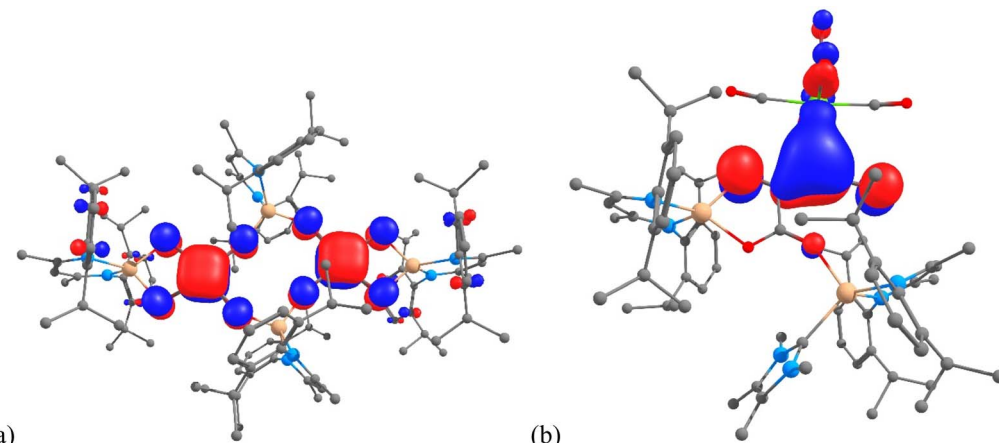


Fig. 5 (a) HOMO-17 of 4, and (b) HOMO-13 of 6, calculated (B3PW91) for the molecules in the gas phase.

ring, giving rise to some C-C π -bond character. The latter is highlighted by the C-C WBI of 1.10. In addition, this delocalisation is clearly seen in the molecular orbitals associated with the squarate fragments (e.g. HOMO-17 in Fig. 5(a); see also Fig. S21 in the ESI[†]). The Mg–O bonds in 4 were found to possess strong donor–acceptor characteristics (while having high ionic character), with donation from the oxygen σ lone pair to an empty Mg orbital, and very little donation from the C–O π bonds. In concert, this results in very low Mg–O WBIs of *ca.* 0.1.

A similar analysis was carried out on compound 6, which incorporates the NHC TMC as a ligand. As was the case with 4, the optimized geometry compares well with that obtained from the X-ray crystallographic analysis. For example, the Mg–C distances are within 0.04 Å, while the Mo–C separations (2.34 vs. 2.331(3) Å) are essentially identical. Moreover, all the C–C and C–O bond distances within the C_4O_4 core of the molecule are well reproduced, with a maximum deviation of 0.01 Å. In line with these bond distances, the NBO analysis clearly indicates the presence of a carboxylate moiety, with the two associated delocalised C–O π -bonds (WBIs = 1.37 and 1.40). The carboxylate moiety is linked to the Mo-coordinated C_3O_2 fragment *via* a C–C single bond (WBI = 0.97). Both C–C interactions within that C_3O_2 unit display significant double bond character (WBIs of 1.37 and 1.62), as is the case for the two C–O bonds in that unit (WBIs of 1.37 and 1.94). Therefore, the C_3O_2 moiety can be seen as a ketenyl unit interacting with Mo through a Mo–C bond that has a WBI of 0.29. While this interaction is not highly covalent, an inspection of the MOs clearly shows a π interaction, associated with HOMO-13 (Fig. 5(b), see also Fig. S22[†]), delocalised over the Mo–C–C unit. The metallo-ketene nature of the complex is also highlighted by the natural charges, which show Mo and the attached ketenyl C-centre to be negatively charged (−1.00 and −0.53, respectively).

Conclusions

In summary, reactions of a dimagnesium(i) compound, activated by simple pyridine or NHC Lewis base coordination, with CO at room temperature, in the presence of one equivalent of $Mo(CO)_6$, led to the reductive tetramerisation of the gas. There

is an apparent competition between the formation of magnesium square and magnesium metallo-ketene products in these reactions, which are not inter-convertible, and have no precedent in the literature. Raising the temperature of these reactions to 80 °C led to the selective formation of the magnesium square, implying that this is the thermodynamic product, while the metallo-ketenes are kinetic products. Computational analyses of the electronic structure of the two product types corroborates electronic delocalization within the squarate complex, as well as the metallo-ketene nature of the molybdenum complexes, as proposed from the experimental data.

The results of this and prior studies show that the degree of magnesium(i) induced reductive oligomerisation of CO, can be readily controlled by altering the method(s) of magnesium(i) reagent activation, ligand steric bulk, and/or the reaction conditions. To date, this has allowed us to selectively access reduced CO dimeric, trimeric, hexameric, and now tetrameric products. With respect to the potential applicability of the latter, s-block metal squarates (*cf.* 4) have, for example, been proposed as electro-active materials (e.g. as anode components in rechargeable batteries),²¹ while s-block metallo-ketenes have very recently been revealed as powerful ketenylation reagents in organic synthesis.²² We continue to explore the selective dimagnesium(i) induced homologation of CO into value-added products and materials, while gaining an understanding of the mechanisms of such reactions, and their relevance to industrial processes utilising CO as a C₁ synthetic building block (e.g. FT).

Experimental section

Full synthetic, spectroscopic and crystallographic details for new compounds; and full details and references for the DFT calculations can be found in the ESI.[†]

Data availability

Crystallographic data for compounds 4–8, *cis*–[$Mo(CO)_4$ (-DMAP)₂] and *cis*–[$Mo(CO)_4$ (TMC)₂] have been deposited at the



Cambridge Crystallographic Database under accessing numbers 2250277–2250283.

Author contributions

K. Yuvaraj and J. C. Mullins performed the synthetic experimental work; K. Yuvaraj, J. C. Mullins and C. Jones interpreted the X-ray diffraction analysis; T. Rajeshkumar, I. Douair and L. Maron performed and interpreted the computational studies; C. Jones conceptualized the research, acquired funding, wrote the manuscript and supervised the work; All authors revised and edited the manuscript. All authors have read and agreed to the published version of the manuscript.

Conflicts of interest

There are no conflicts of interest to declare.

Acknowledgements

CJ thanks the Australian Research Council and the US Air Force Asian Office of Aerospace Research and Development (grant FA2386-21-1-4048). LM is a senior member of the Institut Universitaire de France and thanks the Humboldt Foundation.

Notes and references

- (a) D. Unruh, K. Pabst and G. Schaub, *Energy Fuels*, 2010, **24**, 2634–2641; (b) N. Dahmen, E. Henrich, E. Dinjus and F. Weirich, *Energy Sustain. Soc.*, 2012, **2**, 1–44; (c) S. S. Ail and S. Dasappa, *Renewable Sustainable Energy Rev.*, 2016, **58**, 267–286.
- See for example: (a) *Advances in Fischer–Tropsch Synthesis Catalysts and Catalysis*, ed. B. H. Davis and M. L. Occelli, CRC, Boca Raton, FL, 2009; (b) A. Y. Khodakov, W. Chu and P. Fongarland, *Chem. Rev.*, 2007, **107**, 1692–1744; (c) C. K. Rofer-DePoorter, *Chem. Rev.*, 1981, **81**, 447–474; (d) C. Masters, *Adv. Organomet. Chem.*, 1979, **17**, 61–103.
- See for example: (a) L. D. Durfee and I. P. Rothwell, *Chem. Rev.*, 1988, **88**, 1059–1079; (b) G. Erker, *Acc. Chem. Res.*, 1984, **17**, 103–109; (c) J. A. Gladysz, *Adv. Organomet. Chem.*, 1982, **20**, 1–38; (d) P. T. Wolczanski and J. E. Bercaw, *Acc. Chem. Res.*, 1980, **13**, 121–127; (e) J. M. Parr and M. R. Crimmin, *Angew. Chem., Int. Ed.*, 2023, **62**, e202219203.
- R. Kalesky, E. Kraka and D. Cremer, *J. Phys. Chem. A*, 2013, **117**, 8981–8995.
- (a) R. Y. Kong and M. R. Crimmin, *Dalton Trans.*, 2020, **49**, 16587–16597; (b) S. Fujimori and S. Inoue, *J. Am. Chem. Soc.*, 2022, **144**, 2034–2050.
- (a) K. Yuvaraj, I. Douair, A. Paparo, L. Maron and C. Jones, *J. Am. Chem. Soc.*, 2019, **141**, 8764–8768; (b) N.B. CO homologated products were subsequently shown to be formed in reactions between alkali metal amides and CO or syngas; see, for example, M. Xu, Z.-W. Qu, S. Grimme and D. W. Stephan, *J. Am. Chem. Soc.*, 2021, **143**, 634–638.
- N.B. A related CO trimerization by a β -diketiminato magnesium hydride, yielding a cyclopropantriolate complex, had previously been reported by our group; see: R. Lalrempuia, C. E. Kefalidis, S. J. Bonyhady, B. Schwarze, L. Maron, A. Stasch and C. Jones, *J. Am. Chem. Soc.*, 2015, **137**, 8944–8947.
- O. T. Summerscales, F. G. N. Cloke, P. B. Hitchcock, J. C. Green and N. Hazari, *Science*, 2006, **311**, 829–831.
- (a) O. T. Summerscales, F. G. N. Cloke, P. B. Hitchcock, J. C. Green and N. Hazari, *J. Am. Chem. Soc.*, 2006, **128**, 9602–9603; (b) A. S. Frey, F. G. N. Cloke, P. B. Hitchcock, I. J. Day, J. C. Green and G. Aitkin, *J. Am. Chem. Soc.*, 2008, **130**, 13816–13817; (c) P. L. Arnold, Z. R. Turner, R. M. Bellabarba and R. P. Tooze, *Chem. Sci.*, 2011, **2**, 77–79; (d) S. M. Mansell, N. Kaltsoyannis and P. L. Arnold, *J. Am. Chem. Soc.*, 2011, **133**, 9036–9051; (e) B. M. Gardner, J. C. Stewart, A. L. Davis, J. McMaster, W. Lewis, A. J. Blake and S. T. Liddle, *Proc. Natl. Acad. Sci. U.S.A.*, 2012, **109**, 9265–9270; (f) N. Tsoureas, O. T. Summerscales, F. G. N. Cloke and S. M. Roe, *Organometallics*, 2013, **32**, 1353–1362; (g) I. Castro-Rodriguez and K. Meyer, *J. Am. Chem. Soc.*, 2005, **127**, 11242–11243; (h) A. J. Ryan, J. W. Ziller and W. J. Evans, *Chem. Sci.*, 2020, **11**, 2006–2014.
- K. Yuvaraj, I. Douair, D. D. L. Jones, L. Maron and C. Jones, *Chem. Sci.*, 2020, **11**, 3516–3522.
- N.B. Hill and co-workers subsequently reported the reductive dimerisation of CO to ethynediolate, by reaction with an anionic dimagnesium(i) compound; see: H.-T. Liu, R. J. Schwamm, S. E. Neale, M. S. Hill, C. L. McMullin and M. F. Mahon, *J. Am. Chem. Soc.*, 2021, **143**, 17851–17856.
- A. Paparo, K. Yuvaraj, A. J. R. Matthews, I. Douair, L. Maron and C. Jones, *Angew. Chem., Int. Ed.*, 2021, **60**, 630–634.
- (a) J. Liebig, *Ann. Chem. Pharmacie*, 1834, **11**, 182–189; (b) For an historical overview of this work, see: U. Rosenthal, *Chem. Eur. J.*, 2020, **26**, 14507–14511.
- J. S. Jestilä, Z. Iker, M. J. O. Ryding and E. Uggerud, *Org. Biomol. Chem.*, 2020, **18**, 9499–9510.
- N.B. Although isolated 1:1 THF adduct, $[(\text{DipNacnac})\text{Mg}(\text{THF})(\text{DipNacnac})]$, was not used in this reaction, it is assumed to be transiently formed by loss of THF from the known 2:1 adduct, $[(\text{DipNacnac})(\text{THF})\text{Mg}]_2$, which has been reported to be facile; see (a) S. P. Green, C. Jones and A. Stasch, *Angew. Chem., Int. Ed.*, 2008, **47**, 9079–9083. It is of further note that 1:1 adducts of THF with other dimagnesium(i) compounds have been reported, see: (b) A. J. Boutland, D. Dange, A. Stasch, L. Maron and C. Jones, *Angew. Chem., Int. Ed.*, 2016, **55**, 9239–9243.
- S. P. Green, C. Jones and A. Stasch, *Science*, 2007, **318**, 1754–1757.
- Although no THF adduct of $[(\text{Priso})\text{Mg}–\text{Mg}(\text{Priso})]$ has been isolated, it is assumed that a transient 1:1 THF adduct of the compound is generated in solution; *c.f.* $[(\text{DipNacnac})\text{Mg}–\text{Mg}(\text{THF})(\text{DipNacnac})]$.
- (a) T. Simler, K. N. McCabe, L. Maron and G. Nocton, *Chem. Sci.*, 2022, **13**, 7449–7461; (b) W. J. Evans, J. W. Grate, L. A. Hughes, H. Zhang and J. L. Atwood, *J. Am. Chem. Soc.*, 1985, **107**, 3728–3730; (c) W. J. Evans, D. S. Lee, J. W. Ziller and N. Kaltsoyannis, *J. Am. Chem. Soc.*, 2006, **128**, 14176–



14184; (d) R. J. Ward, I. del Rosal, S. P. Kelley, L. Maron and J. R. Walensky, *Chem. Sci.*, 2023, **14**, 2024–2032.

19 R. Y. Kong and M. R. Crimmin, *J. Am. Chem. Soc.*, 2018, **140**, 13614–13617.

20 As determined from a survey of the Cambridge Crystallographic Database, March, 2023.

21 A. Gosh and S. Mitra, *ChemElectroChem*, 2018, **5**, 159–165.

22 (a) M. Jorges, F. Krischer and V. H. Gessner, *Science*, 2022, **378**, 1331–1336; (b) R. Wei, X.-F. Wang, D. A. Ruiz and L. L. Liu, *Angew. Chem., Int. Ed.*, 2023, **62**, e202219211.

